SOLVENT EFFECTS DURING THE REACTION OF COAL AND BIOMASS MODEL COMPOUNDS IN DENSE WATER

J. R. Lawson, J. R. Obst, M. A. Abraham, S. H. Townsend and M. T. Klein
University of Delaware
Department of Chemical Engineering
Newark, DE 19716

INTRODUCTION

The chemical reactions that accompany the extraction (1) of volatiles from hydrocarbon resources with supercritical water (SCW) are frequently obscured by the complexities of the reaction system. In contrast, the comparative simplicity of model compound structures and product spectra permit resolution of reaction fundamentals (2) and subsequent inference of the factors that control the reactions of real reacting systems. Herein we use model compounds to probe the kinetics of the pyrolysis and solvolysis reactions that likely occur during the extraction of volatiles from coals and lignins.

A previous study of the reaction of guaiacol (orthomethoxyphenol), a mimic of key structural aspects of lignin, in SCW (3) elucidated parallel pyrolysis and hydrolysis pathways, the selectivity to the latter increasing linearly with water density. Guaiacol decomposition kinetics were interestingly nonlinear in water density, which suggested the possibility of unusual cage or solvent effects attributable to dense fluids. We have observed qualitatively similar behavior for the reaction of each of dibenzyl ether (DBE), benzyl phenyl amine (BPA), and benzyl phenyl sulphide (BPS) in SCW and wish to report a candidate reaction network that unifies the previous and present model compound results.

RESULTS

Table I summarizes the reaction conditions of temperature, reactants' concentrations and holding time. Measured amounts of tap water and the commercially available (Aldrich) substrates DBE, BPA and BPS were entered into room temperature stainless steel "tubing bombs" that have been described elsewhere (3). Sealed reactors were immersed into a fluidized sand bath held constant at the desired reaction temperature, which was attained by the reactors in about 2 min; this heat-up period was small compared to ultimate reaction times (up to 40 min) and was, in any case, identical for all runs. Products were identified by GC-MS and quantitated by GC as described elsewhere (3,4).

Neat DBE pyrolysis led to toluene and benzaldehyde as major products along with lesser amounts of benzene and benzyl alcohol. DBE reaction in SCW gave benzyl alcohol, toluene, benzaldehyde and high molecular weight oligomers (4) as major products along with 1,2-diphenylethane, diphenylmethane and triphenylmethane as minor products. The influence of water density (S) on DBE decomposition kinetics is illustrated in Figure 1, where DBE conversion (x) is plotted against water density for parametric values of the reaction time at

374°C. Note that each curve in Figure 1 passes through a minimum value of x; these occurred at about S = 0.4 ± 0.05 in all cases.

Pyrolysis of BPA led to toluene, aniline, benzalaniline and oligomers as major products and minor products including 1,2 diphenylethane and 2-benzylaniline. BPA reaction in water was to benzyl alcohol and benzaldehyde as well as the neat pyrolysis products. The influence of S on BPA reaction kinetics at 386°C is illustrated in Figure 2. For each reaction time illustrated in Figure 2, BPA conversion passes through a minimum as water density increases.

Neat pyrolysis of BPS was to the major product toluene as well as thiophenol, phenyldisulfide, and phenylsulfide. Diphenylmethane and 1-2-diphenylethane were minor products. BPS reaction in water led to all of the neat pyrolysis products except diphenylmethane, as well as minor amounts of benzaldehyde. The influence of S on BPS reaction kinetics at 300°C is illustrated in Figure 3. For each reaction time in Figure 3, BPS conversion passes through a minimum as water density increases.

DISCUSSION

Two experimental observations common to the reaction of each of guaiacol, DBE, BPA and BPS merit summary. First, the overall reaction of each substrate in dense water comprised parallel pyrolysis and solvolysis pathways, with the selectivity to the latter increasing continuously with increasing water density. Second, and for a constant reaction temperature and time, each reactant's conversion passed through a minimum as the water density increased. These observations are consistent with the two complementary mechanistic interpretations that form the basis of the model reaction networks of Figures 4a and 4b. We consider these separately.

In the mechanism represented in Figure 4a, the general reactant R can follow either pyrolysis or solvolysis reaction paths. Neat pyrolytic fragmentation of R to product spectrum $\vec{P_1}$ may, in general, require hydrogen consumption, which will be provided by the reactants themselves. Thus, n of Figure 4a will typically be 3, 0, 1 and 1 for guaiacol, DBE, BPA and BPS, respectively (3,5). Solvolysis to product spectrum $\vec{P_2}$ in Figure 4a is modelled to occur through a solvated reactant intermediate, R^S, that is caged by m water molecules. Increases in water density will shift the overall observed reaction product spectrum from $\vec{P_1}$ (pyrolysis-like) toward $\vec{P_2}$ (solvolysis-like).

Three modelling approximations allowed analytical derivation of a rate expression for the network of Figure 4a. First, reactant solvation was considered to be rapid and in virtual equilibrium at reaction conditions. This is not true during the small heat-up period. Second, solvated reactant molecules were modelled to be caged and thus unable to follow the neat pyrolysis reaction path. Third, the solvated species R^S was considered to exist only at reaction conditions, and ambient analysis by gas chromatography would thus provide the sum $R^* = R + R^S$ as the observable for kinetics analysis.

Eq. 1 is a general rate expression for guaiacol, DBE, BPA and BPS disappearance through the network of Figure 4a; the values of the rate expression parameters will be different for each reactant. For the parameter values listed in Table II, the predictions of Eq. 1 and its integration over time

$$r = \frac{-dR^*}{dt} = \left[\frac{(n+1)k_1}{1 + K_s S^m} + \frac{k_2 S}{(1 + 1/K_s S^m)} \right] R^* \qquad 1)$$

are illustrated in Figures 5a and 5b as plots of the reaction rate and conversion, respectively, as a function of S at a fixed temperature and time. Note the predicted minima are quite general and in accord with the experimental observations. The magnitude and occurrence of these minima are clearly dependent upon the values of rate expression parameters.

In the mechanism of Figure 4b the general reactant R fragments directly through either a pyrolysis or solvolysis pathway to product spectrum $\vec{P_1}$ or $\vec{P_2}$, respectively. The rate constants k_1 and k_2 of Figure 4b include the activation volume pressure dependence, which was not accounted for in Figure 4a; on the other hand, cage effects and thus solvated reactant R^S are absent in Figure 4b. Qualitatively, the overall disappearance rate and conversion will pass through a minimum in pressure, and thus water density, if k_1 decreases faster than k_2S with increases in solvent concentration S. Cage effects in Figure 4a and pressure-dependent rate constants in Figure 4b thus account for the same experimentally observed behavior.

SUMMARY AND CONCLUSIONS

The overall reaction of each of guaiacol, DBE, BPA and BPS in dense water is a superposition of neat pyrolysis and solvolysis reaction pathways. Observed product spectra shift from purely pyrolysis-like to solvolysis-like with increases in water concentration. For a given reaction temperature and time, the reactants' conversions pass through relative minima as the water concentration increases. Two mechanistic interpretations provide consistent predictions. The first comprises parallel pyrolysis and solvolysis reaction pathways, the latter occurring through a solvated reactant intermediate to which pyrolysis is denied. The second is a superposition parallel neat pyrolysis and solvolysis pathway with associated rate constants that are pressure dependent.

ACKNOWLEDGMENT

This work was supported by the U.S. DOE under Grant No. DE-FD22-82PC50799 and the USDA Forest Products Laboratory under Grant No. FP-83-0560.

REFERENCES

(1) Squires, T.G.; Aida, T.; Chen, Y.; Smith, B.F. ACS Div. Fuel Chem. Preprints, 1983, 28, No. 4, 228.

(2) Simmons, M.B.; Klein, M.T. "Free Radical and Concerted Pathways in Dibenzyl Ether Thermolysis"; Ind. Eng. Chem. Fundam. (accepted for publication 1985).

(3) Lawson, J.R.; Klein, M.T. "The Influence of Water on Guaiacol Pyrolysis"; Ind. Eng. Chem. Fundam. (accepted for publication 1984).

(4) Townsend, S.H.; Klein, M.T. "Dibenzyl Ether as a Probe into the Supercritical Fluid Solvent Extraction of Volatiles from Coal with Water"; Fuel (accepted for publication 1985).

(5) Abraham, M.A.; Klein, M.T. "Pyrolysis of Benzyl Phenyl Amine Neat and with Tetralin, Methanol and Water Solvents," I&EC Prod. Res. and Dev. (accepted for publication 1984).

Table 1
Reaction Conditions

Model Compound	Reactant Concentration	Temperature/°C	Holding Time/min
DBE	1.71	374	15
	1.71	374	45
	1.71	374	60
BPA	0.564	386	5
	0.688	386	20
	0.604	386	30
BPS	0.547	300	10
	0.521	300	20

Table 2
Rate Expression Parameters Used in the Prediction of Figure 5

Parameter	Value
n	1
k_1	0.06 sec^{-1}
k_S	1.5 mol^{-1}
m	1
k_2	0.3 sec^{-1} mol^{-1}

Figure 1

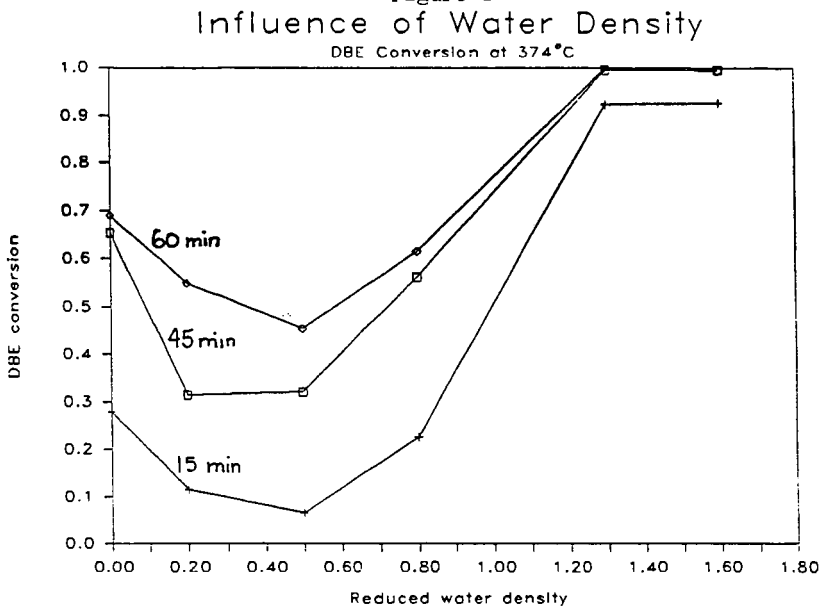

Figure 2
BPA conversion vs. reduced water density
T = 386 C

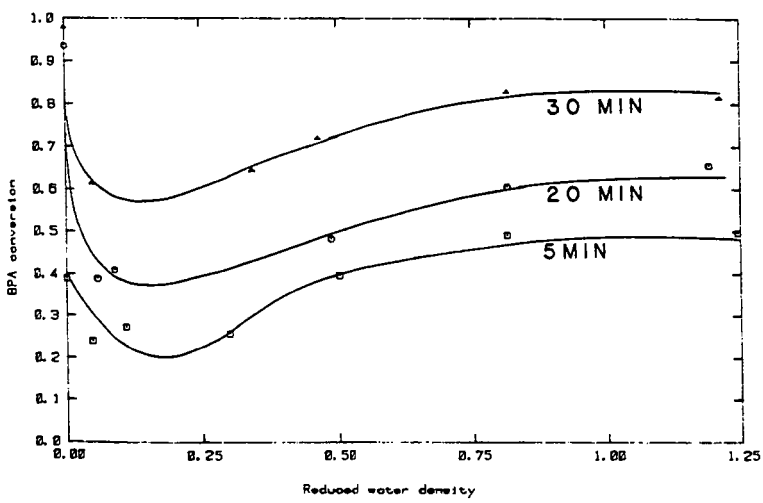

Figure 3
BPS conversion vs. reduced water density
T = 300 C

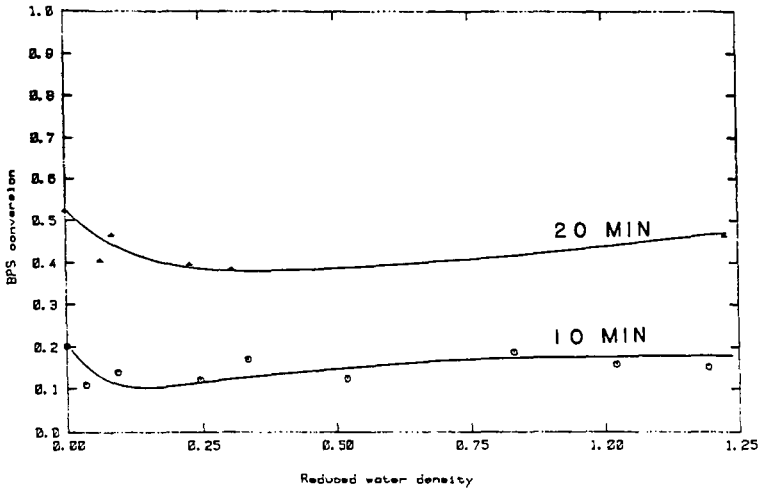

Figure 4: Proposed Reaction Network

Figure 4a: Cage effects

$$\vec{P}_2 \underset{k_2}{\overset{+S}{\leftarrow}} R^S \underset{-mS}{\overset{+mS}{\rightleftarrows}} R \underset{k_1}{\overset{+nR}{\rightarrow}} \vec{P}_1$$

Figure 4b: Pressure-dependent rate constants

$$\vec{P}_2 \underset{k_2}{\overset{+S}{\leftarrow}} R \qquad \underset{k_1}{\overset{+nR}{\rightarrow}} \vec{P}_1$$

Figure 5A
Predicted reaction rates vs.
reduced solvent density

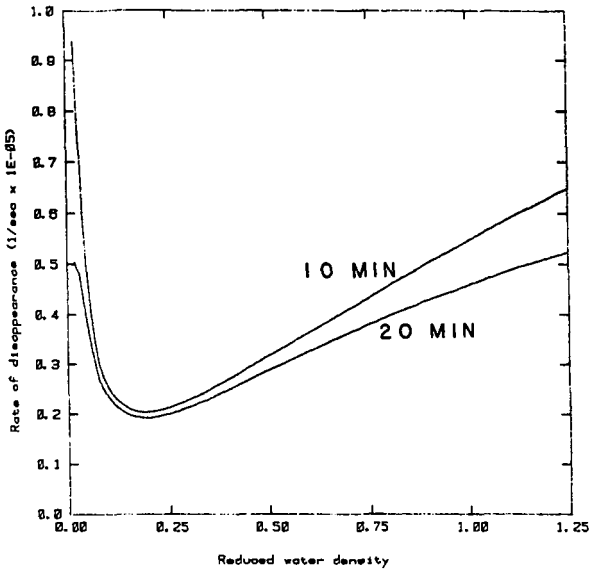
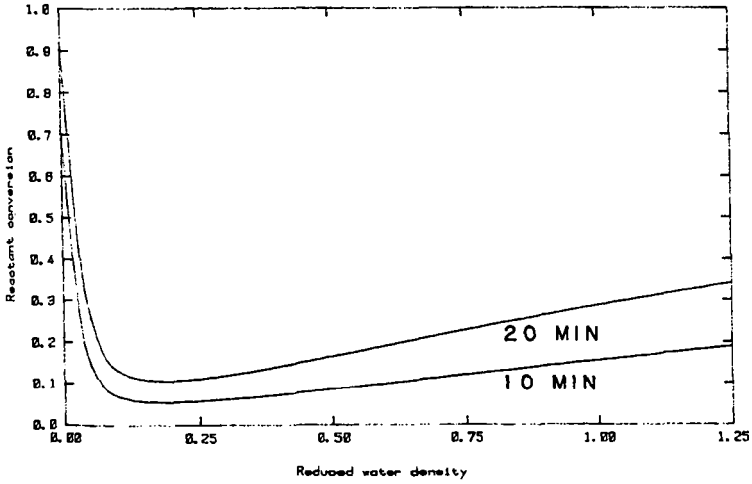
Figure 5B
Predicted conversion vs.
reduced solvent density